Electronic Journal of University of Aden for Basic and Applied Sciences
EJUA-BA Vol. 5 No. 4 (2024)
https://doi.org/10.47372/ejua-ba.2024.4.411
ISSN: 2708-0684

RESEARCH ARTICLE

TREATMENT OF KEROSEN FROM YEMENI – (ALIF FIELD) MARIB CRUDE OIL USING ZEOLITE CATALYST

Mohammed Taha Mohammed[1,2], Rokhsana Mohammed Ismail[3,*], Nadrah M. Hussami[4]

[1] *Dept. of Chemistry, Faculty of Education, University of Aden, Aden, Yemen.*
[2] *Dept. of Health Sciences, Faculty of Medicine and Health Sciences, University of Science and Technology, Aden, Yemen.*
[3] *Dept. of Chemistry, Faculty of Science, University of Aden, Aden, Yemen.*
[4] *Homs Refinery Company, Syria.*

***Corresponding author: Rokhsana Mohammed Ismail; E-mail: ywastd@gmail.com**

Received: 10 December 2024 / Accepted: 15 December 2024 / Published online: 31 December 2024

Abstract

Regarding the investigation of Yemen crude Oil, we found that Marib crude oil was the best one. Based on the information we started to treat Kerosene from Marib Crude Oil using zeolite catalyst because this catalyst is the best one referring to the references. Many bifunctional catalysts in recent studies have been prepared using a single method, it is important to note that different preparation methods can have an influence on their behavior during the process and the properties of the fuels they produce. We used several methods of analysis, such as Catalyst Preparation, Method of Impregnation, Sol – gel Method, in addition we studied Catalyst characterization. The results showed that the acidic sites of Y-zeolites would be thus affecting its catalytic efficiency in reforming process. One of the main reasons for production of higher products was the concentration of Bronsted acid targets in the catalyst. In this study, the catalyst is synthesized the SG method had Bronsted acid sites, resulting in effect of this solvent on their acid sites. Although less jet fuel was produced over the catalyst produced by the IM method (75. 81%), the fuel was higher quality is allowed aromatic and high of naphthens, which were associated with less the Bronsted acid sites of this catalyst.

Keywords: Mareb crude oil, Kerosene, Method of impregnation, Sol gel, Bifunctional catalyst, Physo-chemical properties.

Introduction

Reforming hydrocarbons using zeolites as catalysts shows great potential in producing various oil-based fuels [1, 2]. This method involves using small-sized catalysts to increase the external surface area of the crystals, enabling them to effectively convert large molecules and prevent deactivation [3].

While many bifunctional catalysts in recent studies have been prepared using a single method, it is important to note that different preparation methods can have an influence on their behavior during the process and the properties of the fuels they produce [4, 5].

To achieve a ceramic powder with the desired shape and size, it is important to consider various factors such as pH, reaction temperature, reaction time, and the type of solvent used. To achieve a ceramic powder with the desired shape and size, it is important to consider various factors such as pH, reaction temperature, reaction time, and the type of solvent used [6].

Hence, it is crucial to consider the synthetic strategies employed in catalysts for chemical processes. Catalyst preparation plays a significant role in achieving the desired level of activity and selectivity [7, 8].

In the literature, there are several methods available for incorporating metal into the support. Impregnation (dry or wet), ion exchange, co-precipitation, deposition-precipitation (DP), and sol-gel (SG) are some of the traditional methods used for catalyst preparation that deserve special attention. [9, 10].

Each preparation method has its own set of advantages and disadvantages [11]. For example, deposition-precipitation and sol-gel methods are commonly used techniques for synthesizing nanoparticles. The sol-gel method is particularly effective in achieving proper metal dispersion.

However, this method is typically not suitable for high metal loading because the particles tend to clump together [11] On the other hand, the impregnation (IM) method offers a simple and cost-effective way to produce metal particles that are larger in size and have higher Si/Al ratios.

This approach is suitable for situations where there is a high concentration of metal. The process of reforming operates according to the following mechanism [12].

Alkane Lewis acid → Carbonium ion Brønsted acid → olefin Brønsted acid →

oligomer Bronsted acid → naphthenes Lewis acid → aromatic

Based on this mechanism, both Lewis and Brønsted acid sites contribute to the advancement of the reforming process [4]. Metals act as Lewis acid sites, while the supports provide the Brønsted acid sites.

Hence, including metals in the catalysts becomes necessary to enhance the chemicals involved in these types of processes [13] Additionally, the porosity of the support also plays a role in affecting the dispersion and size of the metal particles [14].

Zeolites, including Y Zeolites, have been widely used in FCC catalysts for over 50 years (since the 1960s). They are favored due to their superior pore volume, pore size, channel length and external surface area compared to other Zeolites [15, 16]. On the other hand,

Cobalt (Co) is often combined with Y zeolite due to its lower cost, greater availability, higher activity, and extensive use in hydrocarbon reforming [17, 18]. However, there are only a few studies comparing Co/Y catalysts that have been prepared using different methods.

Catalytic reforming of kerosene holds great significance as it is extensively used in the production of various types of jet fuels. Kerosene serves as the foundation certain commercial fuels like-A1, as well for the majority of applicable jet propellants as JP-8 and JP-5 [19].

All of these fuels contain four main carbon components, which include normal alkanes, isoalkanes, naphthenes, and acetics [20]. In this, we conducted kerosene reforming experiments Co/Y samples prepared through various synthetic methods.

Several physicochemical properties of the prepared Co/Y samples were characterized to investigate the impact of each synthetic method on the catalytic performance in the reforming process. Moreover, the results of the liquid analysis were interpreted to suggest a more environmentally friendly preparation method. Several physicochemical properties of the prepared Co/Y samples were characterized to investigate the impact of each synthetic method on the catalytic performance in the reforming process. Moreover, the results of the liquid analysis were interpreted to suggest a more environmentally friendly preparation method produce desired fuel.

Experimental part:

Materials:

We obtained cobalt nitrate hexahydrate ($Co(NO_3)_2 \cdot 6H_2O$) and sodium carbonate (Na_2CO_3) from the reputable Merck Company in Germany. Additionally, the Zeolites Company in the USA supplied with commercial Y zeolite (Si/Al = 5. 1 in Na-form, surface area 900 m2 g−1). After distillation in Aden Refinery company, Kerosene was sent to Homs Refinery Company for further analysis such as properties and others. The result listed in Table 1.

Table 1: Specification of kerosene supplied

Property	ASTM Test method	Specification limit	Feed properties
Density at15. 5°C/ kg m $^{-3}$	D 4052	675. 0-740. 0	687. 3
Distillation IBP % Vol at 185 °C % Vol at 200 °C % Vol at 210 °C % Vol at235°C °C FBP	D 86	REP. °C REP. % Vol. REP. %Vol. REP. % Vol. REP. % Vol. 250 °C	146 19. 9 40. 2 % 54. 1% 80. 5 % 201
Sulphur	D 1552	Wt. %	0. 0135
Flash point	D 3828	32 °C min	47
Freezing point	D 2386	-47 °C max	-58
Acidity	D 3242	% Vol	0. 4 ml/0. 5 ml
Aromatic content	D 6379	% Vol	14. 3 %
Olefin content w%		% Vol	0. 24

Catalyst Preparation

Deposition – Precipitation method

To create a 10% Co/NaY sample using the deposition-precipitation method, we add appropriate amounts of 1 M cobalt nitrate ($Co(NO_3)_2 \cdot 6H_2O$) and Na_2CO_3 solutions simultaneously deionized water at a temperature of 70 °C with continuous stirring at a speed of 500-700 rpm and a low flow of basic Na_2CO_3 solution (1 ml min−1) to maintain the pH around 7 ± 0. 2, the mixture was aged under slower stirring (300 rpm) and then filtered.

The sample underwent three washes with deionized water at a temperature of 70 °C before being added to a suspension of Co/Y. The mixtures were stirred at a speed of 300-500 rpm, filtered, and then dried in two steps. Firstly, the sample's temperature was gradually raised from room temperature to 90 °C over a of 2 hours. It was then further increased to 110 °C and kept at this temperature in the air overnight.

Additionally, it also experienced calcination process in a kiln with an initial temperature of 150 °C. This process consisted of three steps:

1) The sample was heated at 150 °C for 10 minutes.
2) The temperature was then gradually increased from 150 to 550 °C in airflow, with a rate of 5 °C per minute.
3) Finally, the temperature was maintained at 550 °C for a duration of 4 hours.

The catalyst created for this purpose was given the designation Co/NaY-DP.

Method of Impregnation

In this approach, a specific quantity of metal was added to the zeolite in the form of an aqueous solution of cobalt nitrate, resulting in the formation of the catalyst Co/NaY-DP.

The desired loading was achieved by drying and calcining the material. To synthesize the catalyst, a wetness impregnation procedure similar to the one described in the literature was used. In this procedure, $Co(NO_3)_2{\cdot}6H_2O$ was added to deionized water.

Afterward, the NaY zeolite was introduced into the solution and gently stirred at a speed of 300–500 rpm at room temperature. Subsequently, it was dried in an set at 110 °C for a duration of 12 hours. Lastly, the catalyst was subjected to calcination in the presence of air at 550 °C with a heating rate of 5 °C per minute for a period of 4 hours. The resulting catalyst was given the designation Co/NaY–IM.

Sol – gel Method

In this approach, a combination of $Co(NO_3)_2 \cdot 6H_2O$ and Y zeolite in a precise ratio needed for a 10% Co/NaY composition was introduced into deionized water. Afterwards, citric acid was added to the prepared aqueous solution to facilitate the chelation of Co^{+2}.

As mentioned in previous works, we added citric acid to the sol at a ratio of two times the number of metal moles. The sol was continuously stirred during this process. The gel was obtained by slowly evaporating the sol at a temperature of 70 °C over a period of 2 hours. Afterward, it was heated to 110 °C and kept at this temperature overnight.

At last, the samples underwent annealing at a temperature of 550 °C for a duration of 4 hours. The resulting catalyst was given the name Co/NaY-SG.

Catalyst characterization

For this study, we employed various techniques to analyze the physical, chemical, and structural components of the Co/Y samples we prepared. We utilized a Philips PW-3710 X-ray diffractometer with a Cu Ka source to record X-ray powder diffraction (XRD) patterns.

The experiment was conducted using Cu-Kα radiation with a wavelength of ƛ= 1. 5418°A. The diffraction patterns were observed in the angle range of 2θ from 5° to 80°, with the scanning rate set at 2° per minute. In order to identify the diffraction patterns, they were compared with those of a known structure found in the Joint Committee of Powder Diffraction Standards (JCPDS) database.

The surface area of the fresh catalysts was determined by conducting a Nitrogen Physisorption analysis using a CHEMBET-3000 surface characterization analyzer (Quantachrome Instruments Company) at a temperature of -77 K.

The surface area was determined using the Brunauer-Emmett-Teller (BET) equation, which takes into account the pressure (P/P0) ranging from 0. 005 to 0. 1. Additionally, the t-plot method was utilized to examine the micro porous characteristics

The distribution of Brønsted and Lewis acid sites in the samples was studied using Fourier transform infrared spectroscopy (FTIR) with a Thermo Nicolet Nexus Model. To begin, a wafer was prepared for the purpose of pyridine adsorption. (scheme. 1)[22].

It was then heated in a vacuum at a temperature of 350 °C and cooled down to the surrounding temperature. The pyridine that was physisorbed underwent degassing at a temperature of 150 °C for 1 hour in a vacuum and was subsequently removed. Finally, the FTIR spectra were prepared.

The concentration of acid sites was determined by analyzing the peak area at 1455 cm−1 for Lewis acid sites and 1545 cm−1 for Brønsted acid sites [22].

Temperature programmed desorption of ammonia (NH3–TP) was conducted with a thermal conductivity detector (TCD), using a BELCAT-M instrument Japan Inc.)

We used NH3–TPD profiles to assess the acidity of the zeolites and prepared catalysts. To obtain these profiles, we heated the samples from 50 to 550 °C at a steady rate of 10 °C per minute, while a flow of helium at 40 ml per minute was maintained.

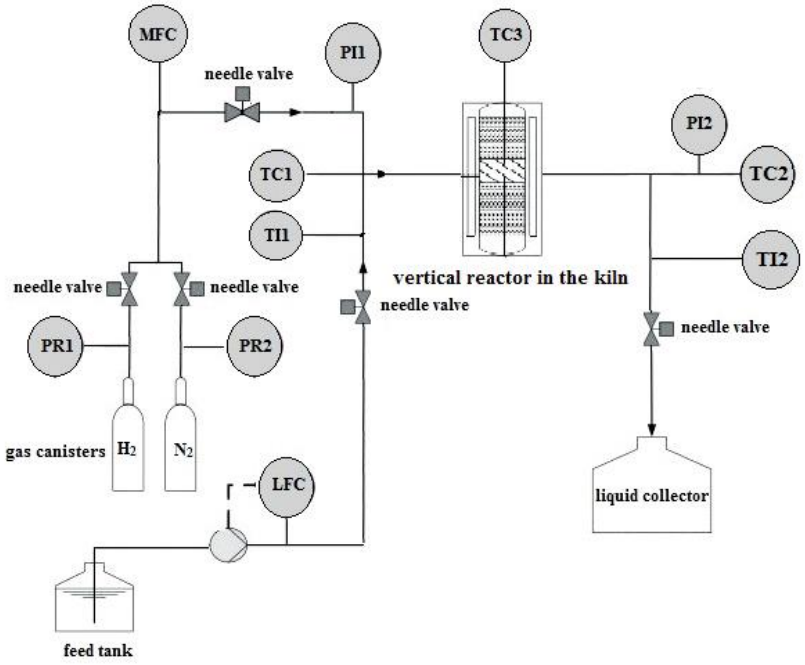

Scheme 1 [22]

Catalytic reforming process

The reaction took place in a fixed-bed reactor made of stainless steel, which had an inner diameter of 10 mm (ID = 10 mm) and a length of 150 mm. The reaction was carried out at a temperature of 450 °C and under atmospheric pressure. In each test, the kerosene reactant was introduced into the setup by controlling its flow rate.

For the first step of the reforming process, we gently placed 1 gram of powdery catalyst, with sizes ranging from 20 to 40 mesh, into the reactor tube. This catalyst occupied approximately 1 centimeter of the reactor's height. To insert the catalyst into the reactor, a metal sieve was used as a bed positioned in the center of a vertical reactor.

The tubular reactor was placed inside a vertical kiln. This kiln provided the necessary energy to achieve the desired reaction temperature (450 °C) for this endothermic process.

The empty space in front of the catalyst bed inside the reactor was helpful in transferring heat and raising the temperature to 450 °C. To eliminate oxygen, the system was purged with N2 flow for 10 minutes at a rate of 70 cc min−1 before the reaction.

The catalyst was then reduced in pure at a temperature of 300 °C for a duration of hours, with flow rate of 50 ml per minute. feed was introduced into the system using the TEC1 peristaltic pump from AQUA, Italy, at a flow rate of5 ml per minute $^{-1}$

The preheater raised the temperature to 300 °C before the reactant entered the reactor. The reactor heating system further increased the temperature to 450 °C, at which the reaction was carried out.

Liquid products were gathered analysis using two-step, and we're finally ready to examine them.

We conducted the analysis of liquid products using an Agilent 6890N gas chromatography (GC) system, which was equipped with a DH capillary column (40 m) and a flame ionization detector (FID). For this approach, a regular solution of typical alkanes (200 parts per million) in n-hexane (C6) was utilized as a solvent. The injection temperature was set at 300 °C for 8 minutes

3. Results and discussion

3. 1 Findings of the textural characteristics

The catalysts that were prepared showed XRD patterns of the Y structure, indicating the zeolite remained intact after incorporating the Co. However, synthesis process did cause a slight change in its crystallinity (Fig. 1)

The XRD patterns of the produced samples and Co/Y zeolite are shown in Figure 2.

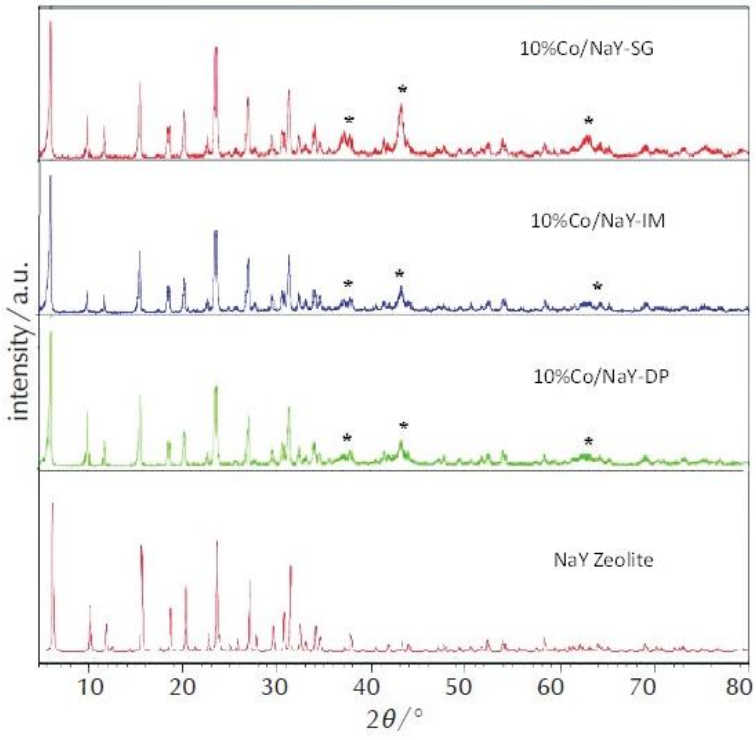

Fig. 1: The XRD patterns of the produced samples and NaY zeolite.

Table 2: Characteristics of Co/Y samples in terms of texture

Row	Sample	Surface area/$m^2 g^{-1}$			Pore volume/$cm^3 g^{-1}$		
		BET [a]	Micropore [b]	External	Total	Micropore[b]	Mesopore
1	Co/Y-DP	580	475	362	0. 45	0. 16	0. 31
2	Co/Y-SG	627	521	394	0. 51	0. 29	0. 21
3	Co/Y-IM	490	383	163	0. 39	0. 14	0. 12

[a]Calculated by BET method, b t-Plot method, c volume at $P/P0 = 0.99$

The XRD pattern revealed the presence of a cubic phase in CoO (JCPDS Card 47-1049) with a lattice constant of a = 4. 1771 Å. The peaks observed at 2θ values of 37. 26°, 43. 29°, 62. 88°, 75. 42°, and 79. 41° corresponded to the diffraction planes of (111), (200), (220), (311), and (222), respectively, indicating the presence of cubic CoO crystals [16, 20].

The literature suggests that when Co/Y samples are reduced, a metal phase is formed. This results in the growth of particles, leading to the formation of larger metal crystallites supported On the outer surface [19], not all the peaks were clearly identified in this study due to some particle sizes being too small for detection by XRD. The distinctive peaks at 2θ of 37. 26°, 43. 29°, and 62. 88° for the Co crystals have been marked with asterisks.

According to Eq. 1, we calculated the average crystal size of different phases by employing the Debye-Scherer[27] equation based on the XRD results.

$$D = \frac{K\lambda}{B\cos\theta} \quad (1)$$

Where k = 0. 89, λ as the wavelength of Cu-Kα radiations, β as the full width at half maximum (FWHM), and θ as the angle obtained from 2θ values corresponding to the maximum intensity peak in the XRD pattern.

In general, there is a direct correlation between the width of the peaks observed in a specific material phase and the average size of the crystallites in that material [21].

Based on the outcomes of the Scherer equation, the estimated dimensions for cobalt oxide nanoparticles in catalysts prepared through sol-gel, deposition-precipitation, and impregnation methods were 6. 988, 8. 986, and 10. 483, respectively. It is worth mentioning that the CoO exhibited a crystalline structure in these findings.

The surface areas and pore volumes of Y zeolites and Co/Y catalysts are shown in Table 2. The Co loading for

the DP, SG, and IM methods was 9. 5, 10. 2, and 9. 8, respectively.

The amounts of the samples were close to what was expected. According to the characterization results, all the samples had a large surface area and were well-characterized, with small crystallite sizes.

3. 2 Acidity characterization

To investigate the distribution of Brønsted and Lewis acid sites in the samples, we employed Py-FTIR using a Thermo Nicolet Nexus Model. In order to carry out pyridine adsorption, a wafer was prepared.

The wafer was then heated to a temperature of 350 °C in a vacuum and subsequently cooled to the surrounding temperature. Physisorbed pyridine was degassed at a temperature of 150 °C for 1 hour in a vacuum and then removed obtain the FTIR spectra. The concentration acid sites was determined by analyzing the peak area at 1455 cm^{-1} for Lewis acid sites and 1545 cm^{-1} for Brønsted acid sites. (Fig. 3)

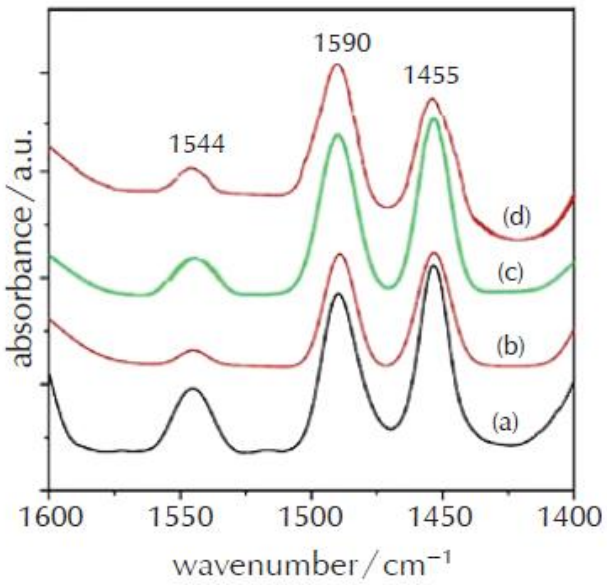

Fig. 2: FTIR spectra (a)NaY, (b) 10% Co/Y-IM, (c) 10% Co/NaY-SG and (d) 10% Co/NaY-DP a

The IR bands observed at 154, 1490, and 1455^{-1} indicate the presence of Brønsted acid sites (B total acidity (B + L), and Lewis sites (L), respectively. When CoO were introduced into NaY zeolite through impregnation (IM), the Brønsted acidity decreased, while the intensity remained high.

The reduction in Brönsted acidity in the SG and DP samples can be attributed to two factors. Firstly, the impregnated sample exhibited crystallinity, which was evident from the XRD and BET results. Secondly, the presence of CoO particles occupied the Brønsted sites.

On the other hand, the addition of CoO particles resulted in an increase in Lewis acidity. Co/Y-SG exhibited the highest B/L (0. 29), while Co/Y-DP showed a moderately high B/L ratio (0. 25), and Co/Y-IM had a relatively lower B/L ratio (0. 10).

For the NH_3-TPD analysis, we began by degassing each sample using a flow of 50 ml min^{-1} helium (He) at a temperature of 550 °C for a duration of 2 hours. Afterward, the sample was cooled down to 100 °C and exposed to a 5 mol% flow of NH_3 gas (balanced by He) for a period of 1 hour.

This was followed by a one-hour flow to remove remaining NH_3. Finally, the sample was gradually heated to 700 °C at a rate of 10 °C per minute using a continuous flow of helium. The results for Y zeolites and Co/Y catalysts were obtained through NH_3-TPD analysis, which are shown in Table 3 and Fig. 3

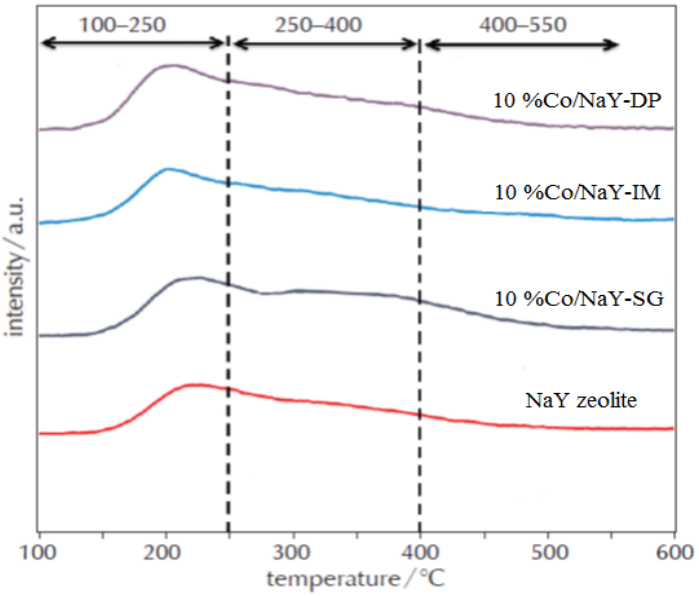

Fig. 3: NH3-TPD profiles for NaY zeolite and the catalysts that were synthesized

As stated in the literature, there are three classifications. Based on the temperature at which ammonia is released, the strength of acid sites can be determined. The acidity is typically categorized into three ranges: 100–250 °C, 250–400 °C, and 400–550 °C. These temperature help in better understanding the acid sites during TPD-NH3 analysis, representing weak, medium, and strong acid sites, respectively [29].

When CoO was modified, some of the acid sites of zeolite Y became covered with CoO particles. This modification introduces medium-strength acidity to the zeolite support. In Figure 4, it can be observed that weak acid sites outnumber strong acid sites in all the samples.

Table 3: Acidity of the catalysts synthesized by the different methods

Row	Sample	NH_3 – TPD acidity/ mmol g^{-1}				P_y– FTIR acidity/ mmol g-1 (at 200 °C			
		Weak	Medium	Strong	Total	Bronsted (B)	Lewis (L)	Total acid (B+L)	B/L Ratio
1	Co/Y-DP	0. 61	1. 86	1. 95	4. 42	0. 38	1. 53	1. 94	0. 25
2	Co/Y-SG	1. 03	1. 51	2. 07	4. 61	0. 49	1. 68	2. 17	0. 29
3	Co/Y-IM	1. 12	0. 89	1. 12	3. 13	0. 12	1. 15	1. 41	0. 10

Table 4: Results of hydrocarbon contents of produced liquids (wt. %)

Row	Catalyst	Method	Alkanes	Isoalkanes	Naphthenes	Aromatic
1	Fresh feed	----	27. 4	27. 9	23. 5	21. 2
2	10% Co/NaY	DP	54. 3	10	3. 4	32. 3
3	10% Co/NaY	IM	35. 6	34. 6	19. 2	10. 6
4	10% Co/NaY	SG	32. 3	37. 3	3	27. 4

Table 5: Results of the product distribution in reforming process

Row	sample	IBP/ °C	EBP/ °C	Gasoline (C5-C15)	Jet fuel (C9-C15)	Diesel (C14-C20)	Lubricant (C19-C25)
1	Co/Y-DP	160	283	10. 56%	86. 91%	2. 53%	0
2	Co/Y-IM	162	285	22. 05%	75. 81%	2. 14%	0
3	Co/Y-SG	158	296	19. 48%	77. 61%	2. 76%	0. 15%

However, it is worth noting that the impregnated sample displayed a lower number of medium and strong acid sites, whereas the sol-gel sample exhibited a higher number of strong acid sites compared to the other samples.

3. 3 Catalyst deactivation discussion

In catalytic works, there are two issues that need to be addressed: reactivation caused by coke and sintering. Typically, coke formation occurs when hydrocarbons are reformed at temperatures above 600 °C. However, in this case, the reaction temperature was 450 °C, which is below the critical temperature (600 °C) for coke formation. Sintering of Co typically happens at temperatures above600 °C; however, the reaction temperature in this research was lower than that. Additionally, the XRD analysis of the catalysts used indicated a low likelihood of sintering. Therefore, there is no need to worry about the catalysts deactivating in this research.

3. 4 Component analysis of the products

Table 4 presents an analysis of the reaction products using the prepared Co/Y catalysts, focusing on four main components: normal alkanes, isoalkanes, naphthenes, and aromatics.

Based on the results observed and previously reported, it can be concluded that catalysts prepared using the DP and IM methods resulted in lighter liquid products compared to those prepared using the SG method.

The use of the DP method in catalyst preparation resulted in the highest aromatic contents compared to the IM or SG methods.

This progress in the reforming process was achieved due to the presence of an appropriate ratio of Lewis and low Brønsted acid sites. This resulted in the conversion of alkanes to carbonium ions, as explained by the reaction mechanism.

The Brønsted acid sites then generate olefins, oligomers, and naphthenes (cyclo paraffins), respectively. Finally, the Lewis acid sites transform naphthenes into aromatics [23]. As a result, having a suitable combination of both types of sites is essential for the advancement of the process.

The catalysts that were prepared successfully transformed the components of kerosene into different types of hydrocarbons. In comparison to other methods of preparation, the Co/Y-SG catalyst exhibited a higher amount of isoalkanes

The activity of this catalyst was primarily influenced by two main factors: the selectivity in siting and the particle size of metal the zeolite cage structure. During the preparation process, the metal atoms could be placed either in the main channel of the zeolites or in the super cages.

Metal ions have the ability to relocate to smaller zeolite cages by eliminating water, a process that occurs during calcination.

Samples that have a lower conversion rate of naphthenes and a higher conversion rate of aromatics result in a desirable liquid. This product is designed to meet the carbon content requirements of jet fuels, ranging from C8 to C18, as well as the aromatic content requirement of 10. 6%. It is important to note that the aromatic limitation is often lower than 25%.

This could be because of its larger particle size, which selectively allows the aromatic components of the feedstock to pass through it during the reforming process.

Additionally, the decrease in crystallinity, as indicated by XRD, has a friendly impact on the activity of the IM catalyst, leading to a more favorable production of naphthenic compounds[1].

3. 5 Catalytic performance of the samples

The hydrocarbons are grouped based on their carbon chain length, which includes gasoline (C5–C10), jet fuel (C9–C15), diesel (C14- C20), and lubricant (C19–C25) [23]. Table 5 shows the distribution of product compositions (%) across all samples in the reform process.

Based on the information Table 5, the liquid product obtained through the DP consisted of 10. 56% gasoline, 86. 91% jet fuel, and 2. 53% diesel hydrocarbon. On the other hand, the products obtained using the IM catalyst had a range of 22. 05% gasoline, 75. 81% jet fuel, and 2. 14% diesel.

The sol-gel method resulted in the production of 19. 48% gasoline, 77. 61% jet fuel, 2. 76% diesel, and 0. 15% lubricant. All catalysts performed exceptionally well, which can be attributed to the excellent structure of the Y zeolite with high crystallinity and a significant number of strong acid sites on its surface.

The formation of isoalkanes was enhanced by both the sol-gel and wetness impregnation methods. However, the liquid produced over Co/NaY-SG had a hydrocarbon range of C8 to C25, indicating the production of heavier hydrocarbons compared to Co/NaY-IM (C8 to C18) and Co/NaY-DP (C8 to C17).

One possible explanation could be the higher level of activity exhibited by the metal particles anchored on the outer surface area. These particular sites were more prevalent when the metal was deposited through impregnation [17, 24, 25, 26].

The reason for the higher gasoline content on the IM catalyst can be attributed to an increased number of Brønsted acid sites. These additional sites assist in the reform process, resulting in the production of lighter components.

This aligns with the cracking reaction mechanism, which requires the presence of Brønsted acid sites to drive the reaction towards increased production of naphthenic components.

This is in line with the cracking reaction mechanism, which relies on the presence of Brønsted acid sites to promote the production of naphthenic components.

Table 6 shows the results of product compositions over the three prepared catalysts.

Table 6: Results of product compositions in reforming process

Row	Distilled product	Compositions of products	Co/Y- DP	Co/Y- IM	Co/Y-SG
1	Gasoline (C5- C10)	Alkanes	5. 00%	26. 13%	42. 73%
		Isoalkanes	54. 59%	39. 96%	41. 78%
		Naphthenes	24. 79%	25. 99%	7. 75%
		Aromatics	15. 62%	31. 42%	7. 74%
2	Jet fuel (C9-C15)	Alkanes	53. 95%	35. 13%	31. 84%
		Isoalkanes	10. 12%	34. 87%	37. 46%
		Naphthenes	3. 01%	19. 30%	3. 45%
		Aromatics	32. 92%	10. 70%	27. 25%
3	Diesel (C14-C20)	Alkanes	22. 9%	23. 14%	12. 42%
		Isoalkanes	38. 49%	41. 38%	23. 98%
		Naphthenes	0	0	0
		Aromatics	38. 62%	35. 48%	63. 60%
4	Lubricant (C19-C25)	Alkanes	0	0	100. 00%
		Isoalkanes	0	0	0
		Naphthenes	0	0	0
		Aromatics	0	0	0

Based on the data in Table 6, it can be observed that as the catalyst's acidity increased, the conversion to naphthenic components decreased. Consequently, the impregnated catalyst with the lowest acidity and highest B/L ratio yielded a higher amount of naphthenes compared to the other catalysts.

Based on the findings, it is evident that the sol-gel method only resulted in a small percentage (0. 15%) of liquids with carbon numbers within the lubricant range. Furthermore, all the products were composed of normal alkanes within this range. Consequently, this product does not meet the specifications of a typical lubricant.

In the reforming process, there was no significant change in the molecular weight distribution. Additionally, the compositions of all products fell within the ranges of the feedstock. The deposition-precipitation method demonstrated an improved capability for the production of jet fuel. The sample that was impregnated resulted in the production of more carbon chains in the gasoline range. However, the impregnated catalysts with higher levels of naphthenes produced hydrocarbons in the jet fuel range that had higher quality. This is because these compositions had a higher energy content.

Conclusion

Co/Y catalysts were successfully synthesized using conventional methods production methods and effect of basic parameters their catalytic efficiency was investigated during the reform process. Kerosene was used raw material (contains 27. 4%) normal alkanes, 27. 9 % isoalkanes, 23. 5 % naphthens and 21. 2 % aromatics). Which was changed during the reform.

The results showed that the acidic sites of Y-zeolites would be thus affecting its catalytic efficiency in reforming process. One of the main reasons for production of higher products was the concentration of Bronsted acid targets in the catalyst.

In this study, the catalyst is synthesized the SG method had Bronsted acid sites, resulting in effect of this solvent on their acid sites. Get up for the B/L ratio, the naphthenic content decreased, and therefore reduced the quality of the jet produced fuels.

Although less jet fuel was produced over the catalyst produced by the IM method (75. 81%), the fuel was higher quality is allowed aromatic and high of naphthens, which were associated with less the Bronsted acid sites of this catalyst.

References

[1] A. Primo, H. Garcia, Zeolites as catalysts in oil refining, chemical society Reviews, Issue 22, 2014 https://pubs.rsc.org/en/content/articlelanding/2014/CS/C3CS60394F

[2] R. M. , Ismail, et al. Catalytic Cracking of Heavy Oil of Alif field- Mareb Yemen, EJUA –BA, v. 2, N. 3, 2021, https://doi. org/10. 47372/ejua-ba. 2021. 3. 104, ISSN: 2708-0684, pp. 103-108.

[3] A. Masalska, J. R. Grzechowiak, K. Jaroszewska, Effect of metal-support interactions in Ni/ZSM-5 + Al_2O_3 catalysts on the transformation of n-Paraffins, Top Catal. 56 (2013) 981–994, doi: https://doi.org/10.1007/s11244-013-0062-x.

[4] P. Yan, J. Mensah, A. Adesina, E. Kennedy, M. Stockenhuber, Highly-dispersed Ni on BEA catalyst prepared by ion-exchange-deposition precipitation for improved hydrodeoxy genation activity, Appl. Catal. B. Environ. 267 (2020) 118690, https://doi.org/10.1016/j.apcatb.2020.118690

[5] Zhenghong Bao, Fei Yu, Catalytic Conversion of Biogas to Syngas via Dry Reforming Process, Advances in Bioenergy, Volume 3, 2018, Pages 43-76.https://doi.org/10.1016/bs.aibe.2018.02.002

[6] G. Prieto et al. Quantitative Relationship between Support Porosity and the Stability of Pore-Confined Metal Nanoparticles Studied on CuZnO/SiO2 Methanol Synthesis Catalysts, 2014, DOI: 10.1021/nn406119j

[7] T. M. Grandprix, Kadja et al, Recent advances in the development of nanosheet zeolites as heterogeneous catalysts, Results in Engineering, Volume 17, March 2023, 100910, https://doi.org/10.1016/j.rineng.2023.100910

[8] H. Lin, Q. L. Liu, Y. B. Dong, Y. H. He, L. Wang, Physicochemical properties and mechanism study of clinoptilolite modified by NaOH, Microporous Mesoporous Mater. 218 (2015) 174–179, https://doi.org/10.1016/j.micromeso.2015.07.017.

[9] K. Klaigaew et al. , Effect of preparation methods on activation of cobalt catalyst supported on silica fiber for Fischer–Tropsch synthesis Chemical Engineering Journal, Volume 278, 15 October 2015, Pages 166-173, https://doi.org/10.1016/j.micromeso.2015.07.017.

[10] S. Mhadmhan et al. Investigation of Ni/SiO2 Fiber Catalysts Prepared by Different methods on Hydrogen production from Ethanol Steam Reforming, Catalysts 2018, 8(8), 319; https://doi.org/10.3390/catal8080319

[11] H. Ruan, Y. Qin, J. Heyne, R. Gieleciak, M. Fenga, B. Yang, Chemical compositions and properties of lignin-based jet fuel range hydrocarbons, Fuel 256 (2019) 115947, doi: https://doi.org/10.1016/j.fuel.2019.115947.

[12] Hadrien Coqueblin et al. Effect of the metal promoter on the performances of H-ZSM5 in ethylene aromatization, Catal. Today 289 (2016) 62–69, https://doi.org/10.1016/j.cattod.2016.08.006.

[13] C. M. Lok et al. Promoted ZSM-5 catalysts for the production of bio-aromatics, a review Renewable and Sustainable Energy ReviewsVolume 113, October 2019, 109248, https://doi.org/10.1016/j.rser.2019.109248

[14] Sotiris Lycourghiotis et al., Nickel catalysts supported on palygorskite for transformation of waste cooking oils into green diesel, Appl. Catal. B Environ. 259 (2019) 118059, https://doi.org/10.1016/j.apcatb.2019.118059

[15] T. K. Habibie, B. H. Susanto, M. F. Carli, Effect of NiMo/zeolite catalyst preparation method for bio jet fuel synthesis, E3S Web of Conferences (2018), https://doi.org/10.1051/

[16] A. Damps, F. Roessner, Oxidative Aromatization of Ethane, European Chemical Sciences Publishing, Research Article, pp. 11 https://doi.org/10.1051/e3sconf/20186702024

[17] Juan SHAO, Ting-jun FU, Jiang-wei CHANG, Wei-li WAN, Rui-yue QI, Zhong LI Effect of ZSM-5 crystal size on its catalytic properties for conversion of methanol to Gasoline, Journal of Fuel Chemistry and Technology, Volume 45, Issue 1, January 2017, Pages 75-83, https://doi. org/10. 1016/S1872-5813(17)30009-9

[18] S. Sartipi, J. E. van Dijk, J. Gascon, F. Kapteijn. Toward bifunctional catalysts for the direct conversion of syngas to gasoline range hydrocarbons: H-ZSM-5 coated Co versus H-ZSM-5 supported Co, Applied Catalysis A: General, Volume 456, 10 April 2013, Pages 11-22, https://doi.org/10.1016/j.apcata.2013.02.012

[19] B. H. Susanto, et. al. Effect of NiMo/Zeolite Catalyst Preparation Method for Bio Jet Fuel Synthesis, E3S Web Conf. Volume 67, 2018, The 3rd International Tropical Renewable Energy Conference “Sustainable Development of Tropical Renewable Energy” (i-TREC 2018), pp. 6 (https://doi.org/10.1051/e3sconf/20186702024

[20] J. L. Weber, C. Hernández Mejía, K. P. de Jong, P. E. de Jongh. Recent advances in bifunctional synthesis gas conversion to chemicals and fuels with a comparison to monofunctional processes, Royal Society of Chemistry, Catal. Sci. Technol. , 2024, 14, 4799- 4842, https://doi.org/10.1039/D4CY00437J, https://pubs.rsc.org/en/content/articlelanding/2024/cy/d4cy00437j

[21] C. M. Lok, J. V. Doorn, G. A. Almansa, Promoted ZSM-5 catalysts for the production of bio-aromatics, a review, Renewable and Sustainable Energy Reviews, Volume 113, October 2019, 109248 https://doi.org/10.1016/j.rser.2019.109248

[22] Report from Homs Refinery Company- Syria pp. 22 copyright of the company

[23] Michael W. J. Glerum, Adam M. Boies, Chapter Three- Reactor processes for value added carbon synthesis and turquoise hydrogen, Advances in Chemical Engineering, Volume 61, 2023, Pages 133-192, https://doi.org/10.1016/bs.ache.2023.04.001 https://www.sciencedirect.com/science/article/abs/pii/S0065237723000029?via%3Dihub

[24] B. Tavakoli, S. Eskandari, et. al, A Review of Preparation Methods for Supported Metal Catalysts Chapter 1, Chunshan Song, editor, Advances in Catalysis, Vol. 61, Burlington: Academic Press, 2017, pp. 1-35, ISBN: 978-0-12-812078-1© Copyright 2017 Elsevier Inc. Academic Pres. https://www.researchgate.net/publication/320972332_A_Review_of_Preparation_Methods_for_Supported_Metal_Catalysts#fullTextFileContent:~:text=DOI%3A%2010.1016/bs.acat.2017.10.001

[25] Y. Zhou, C. Jin, Yong Li, W. Shen, Dynamic behavior of metal Nanoparticles for catalysis Journal of Nonotoday, https://doi.org/10.1016/j.nantod.2018.04.005 https://www.sciencedirect.com/science/article/abs/pii/S174801321730631X?via%3Dihub

[26] J. B. Wagner, et. al, Visualizing the mobility of silver during catalytic soot oxidation, Applied Catalysis B: Environmental, Volume 183, April 2016, Pages 28-36 https://doi.org/10.1016/j.apcatb.2015.10.029 https://www.sciencedirect.com/science/article/abs/pii/S0926337315302095

مقالة بحثية

معالجة الكيروسين من النفط الخام اليمني – مأرب (حقل ألف) باستخدام محفزات الزيوليت

محمد طه محمد[1,2]، رخصانة محمد إسماعيل[3,*]، نادرة محمود الحسامي[4]

[1] قسم الكيمياء، كلية التربية، جامعة عدن، عدن، اليمن.
[2] قسم العلوم الصحية، كلية الطب والعلوم الصحية، جامعة العلوم والتكنولوجيا، عدن، اليمن.
[3] قسم الكيمياء، كلية العلوم، جامعة عدن، عدن، اليمن.
[4] شركة مصفاة حمص، سوريا.

* الباحث الممثل: رخصانة محمد إسماعيل؛ البريد الالكتروني: ywastd@gmail.com

استلم في: 10 ديسمبر 2024 / قبل في: 15 ديسمبر 2024 / نشر في 31 ديسمبر 2024

المُلخّص

استنادا لدراسة نفوط اليمن والتحقق من النتائج وجدنا أن نفط مأرب كان من أفضل أنواع النفط في أغلب القطاعات والحقول. لذلك تم تكرير هذا النفط والحصول على الكيروسين لتتم دراسة جودته باستخدام حافز الزيوليت في مصفاة حمص – سوريا. الكثير من bionfunctional الحفازات استخدمت الطريقة الأحادية، ومن المهم ذكره أن استخدام طرق متعددة لتحضير الحفازات بإمكانها أن تغير سلوك هذه الحفازات. نحن استخدمنا عدة طرق وتحاليل متعددة، مثل تحضير الحفاز بطريقة الغمر (Impregnation – IM)، طريقة Sol. Gel كما تم دراسة خواص هذه الحفازات. النتائج أظهرت المراكز الحمضية للحفاز Y-Zeolite تؤثر بشكل كبير في عملية التحول. كما أن زيادة المنتج يعود إلى تراكيز برونستد الحمضية، على الرغم أن الدراسة قد أظهرت أن طريقة IM تعطي نسبة 75% لوقود الطائرات. الوقود العالي في مكونات المركبات العطرية والنفثينية تؤدي إلى التقليل من مراكز برونستد الحمضية.

الكلمات المفتاحية: نفط خام مأرب، كيروسين، طريقة الغمر **IM**، **Sol. gel**، حفاز **Bifunctional**، خواص الحفازات الفيزيائية الكيميائية.

How to cite this article:

M. T. Mohammed, R. M. Ismail, N. M. Hussami, "TREATMENT OF KEROSEN FROM YEMENI – (ALIF FIELD) MARIB CRUDE OIL USING ZEOLITE CATALYST", *Electron. J. Univ. Aden Basic Appl. Sci.* , vol. 5, no. 4, pp. 543-553, December. 2024. DOI: https://doi.org/10.47372/ejua-ba.2024.4.411